Subsonic Transient Lifting Surface Aerodynamics

T. H. Burkhart*
McDonnell Aircraft Company, St. Louis, Mo.

A method is presented for numerical evaluation of subsonic transient lifting surface aerodynamics. Existing subsonic oscillatory aerodynamic procedures are modified to evaluate generalized aerodynamic forces as two matrices: aerodynamic stiffness and damping. Transfer functions are evaluated numerically which describe the complex variation with reduced frequency of each matrix element. The results are used to formulate the aeroelastic equations of motion in the Laplace operator and real time domains. The Laplace operator formulation is applied to transient flutter solutions, and the results are compared to conventional solutions. The time formulation is applied to several time history dynamic response configurations.

Nomenclature

$\bar{a}$ = complex aerodynamic stiffness load coefficient
$\bar{b}$ = complex aerodynamic damping load coefficient
b_0 = reference semichord
$C_{v\mu}$ = structural viscous damping matrix
e = base of natural logarithm
$f(ik)$ = transfer function
g = structural damping coefficient
h = displacement normal to aerodynamic surface
i = imaginary number
j = index for reduced frequency
k = reduced frequency ($\omega b_0/V$)
$m_{v\mu}$ = generalized mass matrix
$\Delta\bar{p}$ = complex aerodynamic loading
q = generalized coordinate
s = Laplace operator
t = real time
t' = real time
x = streamwise coordinate
$A_{v\mu}$ = steady-state generalized aerodynamic stiffness matrix
$\bar{A}_{v\mu}$ = oscillatory complex generalized aerodynamic stiffness matrix
$B_{v\mu}$ = steady-state generalized aerodynamic damping matrix
$\bar{B}_{v\mu}$ = oscillatory complex generalized aerodynamic damping matrix
C = cost function
$\bar{D}$ = complex aerodynamic influence coefficient matrix
$\bar{E}$ = inverse of complex aerodynamic influence coefficient matrix
F = force
$G_{v\mu}$ = generalized aerodynamic damping matrix (time lagged component)
$H_{v\mu}$ = generalized aerodynamic damping matrix (instantaneous component)
$I_{v\mu}$ = generalized aerodynamic inertia
$J_{v\mu}$ = generalized aerodynamic stiffness matrix (instantaneous component)
$K_{v\mu}$ = structural stiffness matrix
$\bar{K}$ = aerodynamic kernel function
$L_{v\mu}$ = generalized aerodynamic stiffness matrix (time lagged component)
$M^{\epsilon v}$ = inverse of combined structural and aerodynamic inertia matrix
N = number of aeroelastic generalized coordinates
Q_v = total generalized aerodynamic force
$\bar{Q}_v$ = total complex oscillatory generalized aerodynamic force
S = area of aerodynamic surface
V = airspeed
V_r = reference airspeed
$\bar{W}$ = complex oscillatory aerodynamic downwash
Λ^ι = convolution integral of generalized displacement
Ω^ι = convolution integral of generalized velocity
$\alpha_{v\mu_l}$ = time constants for aerodynamic stiffness transfer functions
$\beta_{v\mu_l}$ = time constants for aerodynamic damping transfer functions
ϵ = index for generalized coordinate
ι = index for state variables
μ = index for generalized coordinate
v = index for generalized coordinate
ρ = air density
τ = transfer function time constants
ω = frequency, rad/sec

Presented as Paper 75-758 at the AIAA/ASME/SAE 16th Structures, Structural Dynamics, and Materials Conference, Denver, Colo., May 17-29, 1975; submitted June 4, 1975; revision received March 18, 1976.

Index categories: Aircraft Vibration, Nonsteady Aerodynamics.

*Lead Engineer, Technology – Structural Dynamics.

Introduction

LINEAR unsteady aerodynamic theories used for flutter analysis require that the motion of the aeroelastic configuration be harmonic and that a value for the reduced frequency be specified. The traditional V-g-ω flutter solution satisfies these requirements by solving for the structural damping levels and frequencies required for neutral stability. This solution gives valid stability information and describes the effects of structural damping on the flutter speed; however, each characteristic value of the solution represents a different structural configuration at a different airspeed. The solution does not describe the real dynamic behavior of an aeroelastic configuration at subcritical flutter speeds. Thus, an unsteady aerodynamic representation for transient nonharmonic motion always has been desirable. Such a formulation would make it possible to evaluate real decay rates and frequencies below the onset of flutter to correlate with flight flutter test data. It would be applicable not only to flutter analysis but to an unlimited number of dynamic response problems such as the analysis of combined aeroelastic flight control systems, dynamic loads, gust response. etc. The need for this type of analysis capability has increased because of newer aircraft concepts such as control configured vehicles, flight flutter suppression systems, and gust alleviation systems.

Transient aerodynamic flutter solutions using two-dimensional aerodynamics have been in general use for some time. The work of Richardson,[1] Rodden and Stahl,[2] and Ferman et al.[3] are some of the many examples. These methods usually consider a Laplace approximation for the oscillatory

circulation function such as Wagner's function. This allows the equations of motion to be expressed with Laplace operators; thus, constant airspeed stability analyses are possible, resulting in real frequencies and decay rates. For example, the method of Ref. 3 has been applied successfully to the flutter data correlation and flutter margin estimation presented in the flight flutter test report of Ref. 4. It has been used to formulate the aeroelastic equations of motion in the time history simulation of the combined aeroelastic flight control system presented in Ref. 5. The program of Ref. 5 allows a nonlinear representation of the control system and is being used for the design and analysis of active flutter control systems as presented by Triplett et al.[6]

With three-dimensional lifting surface aerodynamic theories, the transient aerodynamic formulation becomes more complicated. Iterative schemes such as the *p-k* method by Hassig[7] successfully evaluate real decay rates and frequencies for flight flutter data correlation and can be used with lifting surface aerodynamics. These methods are not, however, applicable to time history dynamic force response anslysis. The method to be presented prepares a set of generalized aerodynamic force matrices and transfer functions based upon harmonic data from existing lifting surface methods. The results are used to formulate the aeroelastic equations of motion with respect to both Laplace operators and real time. The formulation is applied to transient flutter solutions and time history simulations, and the numerical results are presented.

Theoretical Development

Overview

This numerical method starts with any subsonic lifting surface oscillatory aerodynamic computer program. Either the kernel function methods as formulated by Rowe[8] or Cunningham[9] or the doublet lattice method as formulated by Albano and Rodden[10] and Rodden et al.[11] may be used. The selected lifting surface aerodynamic program is modified to evaluate the generalized aerodynamic forces in two parts, which will be referred to as generalized stiffness forces and generalized damping forces. These modifications do not limit the original configuration applicability of the program. These aerodynamic forces are calculated for a set of reduced frequencies which cover the required frequency range and include the steady-state zero value. Then, transfer functions are evaluated which describe the variation of each complex force element with reduced frequency. A transfer function is selected which can be transferred readily to the time and operator domains, using the Fourier and Laplace transforms. The procedures for evaluating the aerodynamic matrices and transfer functions along with their implementation in equations of motion are as follows.

Evaluation of Aerodynamic Forces

Subsonic lifting surface methods are based upon the integral equation which relates the normal downwash momentum, caused by the motion of the aerodynamic surface, to the pressure loading. For the downwash caused by the generalized coordinate q, this integral equation is

$$\frac{\partial \bar{W}}{\partial q} = \int\int \frac{\partial \Delta \bar{p}}{\partial q} \bar{K} ds \tag{1}$$

The symbols with the bar (e.g., $\bar{W}$) are complex quantities. The solution to Eq. (1) is by collocation and results in the complex matrix equation

$$\left[\frac{\partial \bar{W}}{\partial q}\right] = [\bar{D}]\left[\frac{\partial \Delta \bar{p}}{\partial q}\right] \tag{2}$$

where the $\partial \bar{W}/\partial q$ is known from the motion of the aerodynamic surface and $\partial \Delta \bar{p}/\partial q$ represents the aerodynamic loading to be evaluated. The $\partial \Delta \bar{p}/\partial q$ matrix may represent the aerodynamic loading in various ways; for kernel function methods the $\partial \Delta \bar{p}/\partial q$ matrix denotes pressure mode coefficients, whereas for doublet lattice methods the $\partial \Delta \bar{p}/\partial q$ matrix denotes the constant load over a finite element panel. The $\bar{D}$ matrix is evaluated according to the method selected.

The matrix $[\partial \bar{W}/\partial q]$ is determined by evaluating the downwash at a set of locations on the surface (i.e., collocation points or finite element panels). This matrix is defined in terms of the motion of the aerodynamic surface as

$$\left[\frac{\partial \bar{W}}{\partial q}\right] = \rho V^2 \left[\frac{\partial^2 h}{\partial x \partial q} + \frac{ik}{b_0}\frac{\partial h}{\partial q}\right] \tag{3}$$

Then the aerodynamic loads are calculated by solution of Eq. (2). Let

$$[\bar{D}]^{-1} = [E_R] + i[E_I] \tag{4}$$

then, by matrix multiplication

$$\left[\frac{\partial \Delta \bar{p}}{\partial q}\right] = \rho V^2 \left\{ [E_R]\left[\frac{\partial^2 h}{\partial x \partial q}\right] - [E_I]\left[\frac{k}{b_0}\frac{\partial h}{\partial q}\right] + i[E_I]\left[\frac{\partial^2 h}{\partial x \partial q}\right] + i[E_R]\left[\frac{k}{b_0}\frac{\partial h}{\partial q}\right] \right\} \tag{5}$$

From Eq. (5) it can be seen that the variation of the complex aerodynamic loading with reduced frequency is determined by the individual variations of the $[\bar{D}]$ matrix and the downwash matrix. The $\bar{D}$ matrix variation is consistent for all modes of dynamic motion. The downwash matrix variation with reduced frequency is determined by the relative values of the modal slopes ($\partial^2 h/\partial x \partial q$) and model displacements ($\partial h/\partial q$) and, thus, is different for each dynamic mode. For example, the load caused by a pure bending mode starts out at low reduced frequencies with 90° phase lead over those caused by a pure twisting mode. Thus, for normal mode shapes, the variation of the aerodynamic loading with reduced frequency is different for each mode. In order to obtain a more uniform complex variation for all mode shapes, the loads due to modal slope are handled separately from the loads due to displacement. In addition, the reduced frequency (ik) is factored from the displacement downwash component. This rotates the displacement loads back to 90° and allows evaluation at the zero value of reduced frequency. The aerodynamic load coefficients now are expressed as two complex quantities.

1) Aerodynamic Stiffness Load Coefficients

$$\left[\frac{\partial \bar{a}}{\partial q}\right] = \left[E_R + iE_I\right]\left[\frac{\partial^2 h}{\partial x \partial q}\right] \tag{6}$$

2) Aerodynamic Damping Load Coefficients

$$\left[\frac{\partial \bar{b}}{\partial q}\right] = [E_R + iE_I]\left[\frac{l}{b_0}\frac{\partial h}{\partial q}\right] \tag{7}$$

Thus, Eq. (5) can be rewritten

$$\left[\frac{\partial \Delta \bar{p}}{\partial q}\right] = \rho V^2 \left\{ \left[\frac{\partial \bar{a}}{\partial q}\right] + ik\left[\frac{\partial \bar{b}}{\partial q}\right] \right\} \tag{8}$$

The total generalized force derivatives for loads due to the μth coordinate doing work on the υth coordinate are defined as follows:

$$\bar{Q}_{\upsilon\mu} = \int\int \left(\frac{\partial \Delta \bar{p}}{\partial q^{\mu}}\right)\left(\frac{\partial h}{\partial q^{\upsilon}}\right) dS \tag{9}$$

Using Eq. (8)

$$\bar{Q}_{v\mu}=\rho V^2\iint\left[\left(\frac{\partial\bar{a}}{\partial q^\mu}\right)+ik\left(\frac{\partial\bar{b}}{\partial q^\mu}\right)\right]\left(\frac{\partial h}{\partial q^v}\right)dS \tag{10}$$

Then, the generalized force derivatives can be separated into the following two matrices:

1) Aerodynamic Stiffness Force Derivatives

$$\bar{A}_{v\mu}=\iint\left(\frac{\partial\bar{a}}{\partial q^\mu}\right)\left(\frac{\partial q}{\partial q^v}\right)dS \tag{11}$$

2) Aerodynamic Damping Force Derivatives

$$\bar{B}_{v\mu}=\iint\left(\frac{\partial\bar{b}}{\partial q^\mu}\right)\left(\frac{\partial h}{\partial q^v}\right)dS \tag{12}$$

The $\bar{A}_{v\mu}$ is not precisely an aerodynamic stiffness matrix, since it contains some damping, and the $\bar{B}_{v\mu}$ is not precisely a damping matrix, since it contains the aerodynamic inertia.

The method requires that the $\bar{A}_{v\mu}$ and $\bar{B}_{v\mu}$ matrices be evaluated at a set of reduced frequencies including the zero value. For the zero value, the $A_{v\mu}(k=0)$ matrix represents the steady state generalized force derivative matrix. The $B_{v\mu}(k=0)$ represents a pseudo-steady-state generalized damping derivative matrix. The elements of the matrices at each reduced frequency are normalized by their respective steady-state values. These normalized matrices are made up of complex elements whose variations with reduced frequency start at a real value of one for zero reduced frequency. Then, with increasing reduced frequency, the elements move smoothly into the first or fourth quadrants of the complex plane. Figures 1-3 present numerical examples of this type of data.

The next step is to develop an analytical transfer function which will approximate the variation of each complex element with reduced frequency. Such a transfer function would allow the aerodynamic matrices to be expressed as follows

$$\bar{A}_{v\mu}(ik)=A_{v\mu}(k=0)\,f_{Av\mu}(ik) \tag{13a}$$

$$\bar{B}_{v\mu}(ik)=B_{v\mu}(k=0)\,f_{Bv\mu}(ik) \tag{13b}$$

The transfer function formulation selected was

$$f=\frac{1+\tau_1 ik+\tau_2(ik)^2}{1+|\tau_3|\,ik} \tag{14}$$

This transfer function satisfies the following requirements:

1) It goes to a value of one as k goes to zero.

2) It is the minimum order transfer function capable of satisfactorily approximating the complex variation of a typical aerodynamic force element with reduced frequency.

3) It can be transformed readily to a time or Laplace operator formulation.

4) It represents a stable system. This is satisfied by requiring τ_3 to be positive.

The last requirement, that τ_3 must be positive for a stable transfer function, creates considerable difficulty in selection of a numerical procedure to evaluate the time constants from the given lifting surface program data. Such a constraint eliminates possibilities for least-squares curve fitting. The method finally selected was a gradient cost function optimization algorithm.

The procedure starts with a set of normalized complex aerodynamic force elements and corresponding reduced frequencies: $A_R(k_j)$, $iA_I(k_j)$, k_j. A cost function is defined as the total square deviation between the original data and the transfer function

$$C=\sum_j\left[A_R(k_j)+iA_I(k_j)-f(ik_j)\right]^2 \tag{15}$$

The gradient algorithm is used to find the values for the τ constants that minimize this cost function. Thus, a transfer function is evaluated which fits the original data and, at the same time, imposes the constraint of a positive τ_3. The mathematical steps of the gradient algorithm are described in Ref. 12, along with several other algorithms available for cost optimization. The gradient algorithm is one of the least sophisticated of the optimization procedures, but it was found to be the most dependable for this particular problem.

After evaluation of the transfer functions, the total generalized aerodynamic forces can be expressed in terms of the transfer function time constants and steady-state force matrices

$$\bar{Q}_v=\rho V^2\left[A_{v\mu}(k=0)\,\frac{1+\alpha_{v\mu1}ik+\alpha_{v\mu2}(ik)^2}{1+\alpha_{v\mu3}ik}\right.$$
$$\left.+ik\,B_{v\mu}(k=0)\,\frac{1+\beta_{v\mu1}ik+\beta_{v\mu2}(ik)^2}{1+\beta_{v\mu3}ik}\right]q^\mu \tag{16}$$

Note that ik, originally factored from the modal displacement part of the downwash of Eq. (3), has been returned as a multiplier of the aerodynamic damping terms in Eq. (16).

After algebraic expansion of the transfer function, transformation to dimensional frequency, and application of the inverse Fourier transform, the aerodynamic forces can be expressed using real time integrals and derivatives of the generalized coordinates. This has the following form

$$Q_v=\rho I_{v\mu}\ddot{q}^\mu+\rho VH_{v\mu}\dot{q}^\mu+\rho V^2J_{v\mu}q^\mu$$
$$+\rho V^2G_{v\mu}\int_o^t\dot{q}^\mu\exp\left(-\frac{V}{b_o}\,\frac{t-t'}{\beta_{v\mu3}}\right)dt'$$
$$+\rho V^3L_{v\mu}\int_o^t q^\mu\exp\left(-\frac{V}{b_o}\,\frac{t-t'}{\alpha_{v\mu3}}\right)dt' \tag{17}$$

where

$$I_{v\mu}=b_o^2B_{v\mu}\left(\frac{\beta_{v\mu2}}{\beta_{v\mu3}}\right) \tag{18a}$$

$$H_{v\mu}=b_o\left[A_{v\mu}\frac{\alpha_{v\mu2}}{\alpha_{v\mu3}}+B_{v\mu}\left(\frac{\beta_{v\mu1}}{\beta_{v\mu3}}-\frac{\beta_{v\mu2}}{\beta_{v\mu3}^2}\right)\right] \tag{18b}$$

$$J_{v\mu}=A_{v\mu}\left(\frac{\alpha_{v\mu1}}{\alpha_{v\mu3}}-\frac{\alpha_{v\mu2}}{\alpha_{v\mu3}^2}\right) \tag{18c}$$

$$G_{v\mu}=B_{v\mu}\left(\frac{1}{\beta_{v\mu3}}-\frac{\beta_{v\mu1}}{\beta_{v\mu3}^2}+\frac{\beta_{v\mu2}}{\beta_{v\mu3}^3}\right) \tag{18d}$$

$$L_{v\mu}=\frac{A_{v\mu}}{b_o}\left(\frac{1}{\alpha_{v\mu3}}-\frac{\alpha_{v\mu1}}{\alpha_{v\mu3}^2}+\frac{\alpha_{v\mu2}}{\alpha_{v\mu3}^3}\right) \tag{18e}$$

The I matrix is analogous to aerodynamic inertia. The H and J matrices determine aerodynamic damping and stiffness forces. The G and L matrices determine aerodynamic damping and stiffness forces that have a time lag relative to the generalized velocities and displacements, respectively.

Equations of Motion

Equation (17) represents the unsteady aerodynamic forces for arbitrary generalized motion of an aeroelastic system at a constant airspeed. This equation now can be included in the complete equations of motion:

$$(m_{v\mu}-\rho I_{v\mu})\ddot{q}^\mu+(C_{v\mu}-\rho VH_{v\mu})\dot{q}^\mu$$
$$+(K_{v\mu}-\rho V^2J_{v\mu})q^\mu-\rho V^2G_{v\mu}\int_o^t\dot{q}^\mu\exp\left(-\frac{V}{b_o}\,\frac{t-t'}{\beta_{v\mu3}}\right)dt'$$
$$-\rho V^3L_{v\mu}\int_o^t q^\mu\exp\left(-\frac{V}{b_o}\,\frac{t-t'}{\alpha_{v\mu3}}\right)dt'=F_v \tag{19}$$

The quantities $m_{v\mu}$, $C_{v\mu}$, and $K_{v\mu}$ are the inertia, viscous damping, and stiffness matrices of the structure, and the quantity F_v is the component of an arbitrary applied force doing work on the q^v generalized coordinate. The convolution integrals of Eq. (19) can be handled by introducing a set of state variables. For a system of N degrees of freedom, there are two sets of N^2 number of variables which are defined as

$$\Lambda^\iota = \int_o^t q^\mu \exp\left(-\frac{V}{b_o}\frac{t-t'}{\alpha_{v\mu 3}}\right) dt' \tag{20a}$$

$$\Omega^\iota = \int_o^t \dot{q}^\mu \exp\left(-\frac{V}{b_o}\frac{t-t'}{\beta_{v\mu 3}}\right) dt' \tag{20b}$$

where the index ι is determined by the following formula:

$$\iota = v + N(\mu - 1) \tag{21}$$

These variables are defined in differential form by the following:

$$\dot{\Lambda}^\iota = q^\mu - \left(\frac{V}{b_o \alpha_{v\mu 3}}\right)\Lambda^\iota \tag{22a}$$

$$\dot{\Omega}^\iota = \dot{q}^\mu - \left(\frac{V}{b_o \beta_{v\mu 3}}\right)\Omega^\iota \tag{22b}$$

The integrals of Eq. (20) are the nonhomogeneous solutions to the differential Eq. (22). In control system terminology this is equivalent to representing the integrals as additional feedback loops for each state variable. For a time history solution, Eq. (22) must be integrated simultaneously with the basic equations of motion which now are expressed in terms of the generalized coordinates and the feedback state variables. The lagged aerodynamic stiffness and damping matrices are reorganized to $N \times N^2$ size by the following

$$L_{v\iota} = L_{v\iota}, \quad G_{v\iota} = G_{v\mu} \quad \text{if} \quad \iota = v + N(\mu - 1) \tag{23a}$$

$$L_{v\iota} = 0, \quad G_{v\iota} = 0 \quad \text{if} \quad \iota \neq v + N(\mu - 1) \tag{23b}$$

Then, after inverting the combined structural and aerodynamic inertia matrix

$$[M^{\mu v}] = [m_{v\mu} - \rho I_{v\mu}]^{-1} \tag{24}$$

the equations of motion are of the following form

$$\ddot{q}^\epsilon = -M^{\epsilon v}[(C_{v\mu} - \rho V H_{v\mu})\dot{q}^\mu + (K_{v\mu} - \rho V^2 J_{v\mu})q^\mu - \rho V^2 G_{v\iota}\Omega^\iota - \rho V^3 L_{v\iota}\Lambda^\iota - F_v] \tag{25}$$

where the ranges of the indices are ϵ, v, $\mu = 1,2,\ldots N$; $\iota = 1,2,\ldots N^2$.

Equation (25) is appropriate for simulating the aeroelastic configuration in any type of time history dynamic analysis. The time lags which occur in the growth of the aerodynamic loads are represented readily by simultaneously including the feedback differential equations of Eq. (22) in the analysis. The formulation provides for an arbitrary force input. This force can be used to represent a variety of dynamic forces such as control system actuator inputs, gust loads, landing gear impact, etc. Equations (22) and (25) are in a form suitable for application on an analog computer or on a digital computer using a dynamic simulation language such as those described in Refs. 13 and 14. The state variable equations of the control system with any nonlinearites can be included in these types of time simulations.

Transient Flutter Solution

To obtain a transient flutter stabilility analysis at a constant airspeed, the equations of motion can be expressed in the Laplace operator domain. The Laplace transforms of Eqs. (22) and (25) have the following form, provided that all of the initial conditions of the generalized coordinates are zero

$$(m_{v\mu} - \rho I_{v\mu})s^2 q^\mu + (C_{v\mu} - \rho V H_{v\mu})sq^\mu + (K_{v\mu} - \rho V^2 J_{v\mu})q^\mu - \rho V^2 G_{v\iota}\Omega^\iota - \rho V^3 L_{v\iota}\Lambda^\iota = F_v \tag{26a}$$

$$s\Lambda^\iota + \left(\frac{V}{b_o \alpha_{v\mu 3}}\right)\Lambda^\iota - q^\mu = 0 \tag{26b}$$

$$s\Omega^\iota + \left(\frac{V}{b_o \beta_{v\mu 3}}\right)\Omega^\iota - sq^\mu = 0 \tag{26c}$$

These equations can be used for flutter stability analysis by setting the external force F to zero, specifying a value for airspeed and air density, and calculating the characteristic values of the system of equations. Equation (26) can be assembled as a dynamic matrix for purposes of extracting the characteristic values. Again, using the inverse of the combined structural and air inertia as defined in Eq. (24), the assembled dynamic matrix has the form indicated in Eq. (27).

The characteristic values are obtained for this dynamic matrix by routine computer procedures. The number of characteristic values is $2(N^2 + N)$. Of these values, there are $2N$ number of characteristics roots which are complex conjugate pairs representing the aeroelastic configuration. The other $2N^2$ number of characteristic roots are latent aerodynamic roots associated with the feedback state variables. They are always stable and either real or complex with a small imaginary magnitude. With some knowledge of the structural frequencies, the aeroelastic roots can be sorted readily from the latent aerodynamic roots.

It is possible to use Eq. (26) for stability analysis of aeroelastic configurations with the flight control system. This can be readily done by combining the linearized control system state variable equations, as formulated in the Laplace

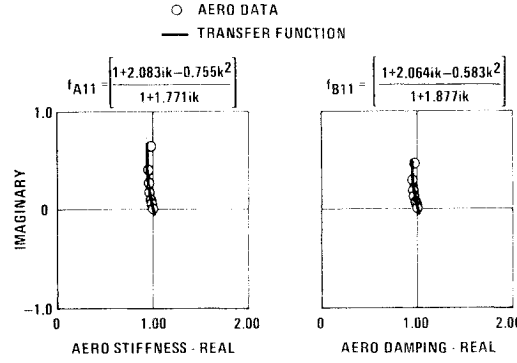

Fig. 1 Comparison of aerodynamic transfer functions to original aerodynamic data for D/F codes = 1, 1.

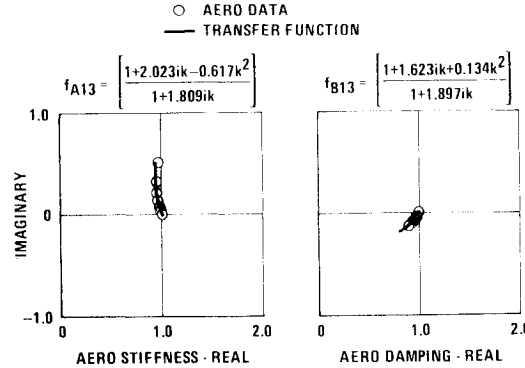

Fig. 2 Comparison of aerodynamic transfer functions to original aerodynamic data for D/F codes = 1, 3.

domain, with the aeroelastic equations of motion. Extraction of characteristic values can be performed by an assembly of a dynamic matrix similar to that of Eq. (27) with the control system variables included as degrees of freedom

$$s\begin{Bmatrix}\Lambda\\ \Omega\\ q\\ sq\end{Bmatrix}=\left[\begin{array}{c|c|c|c}-(V/b_0\alpha_3) & 0 & \begin{matrix}\{I\}\\ & \{I\}\\ & & \ddots\\ & & & \{I\}\end{matrix} & 0\\ \hline 0 & -(V/b_0\beta_3) & 0 & \begin{matrix}\{I\}\\ & \{I\}\\ & & \ddots\\ & & & \{I\}\end{matrix}\\ \hline 0 & 0 & 0 & \begin{matrix}I\\ & I\\ & & \ddots\\ & & & I\end{matrix}\\ \hline \rho V^3ML & \rho V^3ML & M[-K+\rho V^2J] & M[-C+\rho VH]\end{array}\right]\begin{Bmatrix}\Lambda\\ \Omega\\ q\\ sq\end{Bmatrix} \tag{27}$$

Applications

Several applications of this procedure are presented. The calculations include the evaluation of aerodynamic transfer functions and their application to transient flutter analyses and to time history dynamic response analyses. A contemporary aircraft aeroelastic configuration is used for these studies. It has a planform with an aspect ratio of 3, a leading-edge sweep of 45°, and a trailing-edge control surface. The generalized coordinates are the first four normal vibration modes and control surface rotation. All of the original harmonic aerodynamic data were evaluated using the subsonic kernel function method of Ref. 15 with a Mach number of 0.6.

Aerodynamic Transfer Functions

Figures 1-3 present a comparison of the calculated aerodynamic transfer functions to the original kernel function program data. The symbols denote the original data which have been normalized to their respective $k=0$ values. The data correspond to reduced frequencies of 0, 0.2, 0.3, 0.5, 0.7, 1, and 1.5. The line indicates the transfer function. The transfer function time constants are indicated in the equations on each plot. The degrees-of-freedom codes indicate the element of the aerodynamic matrices represented. For example, a code (1, 3) designates the aerodynamic loads due to the third vibration mode working on the first vibration mode. From these figures, it is seen that the transfer functions calculated are excellent approximations of the original lifting surface program data. These transfer functions along with the $k=0$ stiffness and damping matrices define the transient generalized aerodynamic data set.

Transient Flutter Analysis

The transient aerodynamics have been applied to flutter analyses (i.e., Laplace operator formulation). The flutter analysis using four normal modes, without a control surface, is presented in Fig. 4. The results are shown as the variation in equivalent structural damping and frequency with airspeed ratio (V/V_r). The transient solution results are compared with the conventional V-g-ω solution results. The circled data represent the V-g-ω solution results, and the curves represent the transient solutions which were performed at 0.1 V/V_r intervals. At the flutter crossings (corresponding to pure harmonic motion), both the transient flutter solution and the V-g-ω solution should agree. The data of Fig. 4 show excellent agreement between the transient and V-g-ω solutions at both neutral stability points.

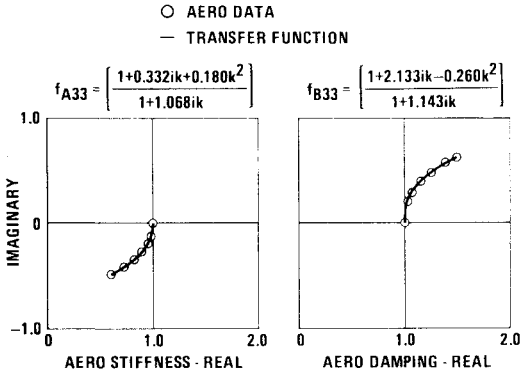

Fig. 3 Comparison of aerodynamic transfer functions to original aerodynamic data for D/F codes = 3, 3.

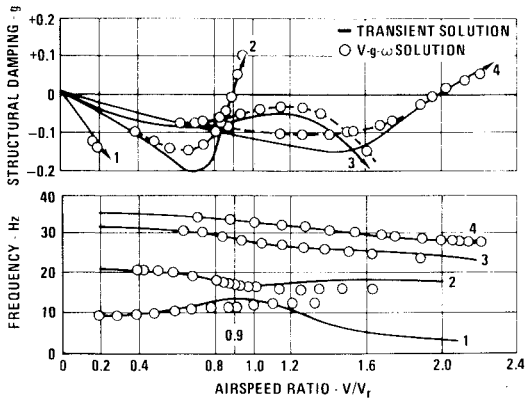

Fig. 4 Comparison of transient and V-g-ω flutter solution for four-degree-of-freedom wing.

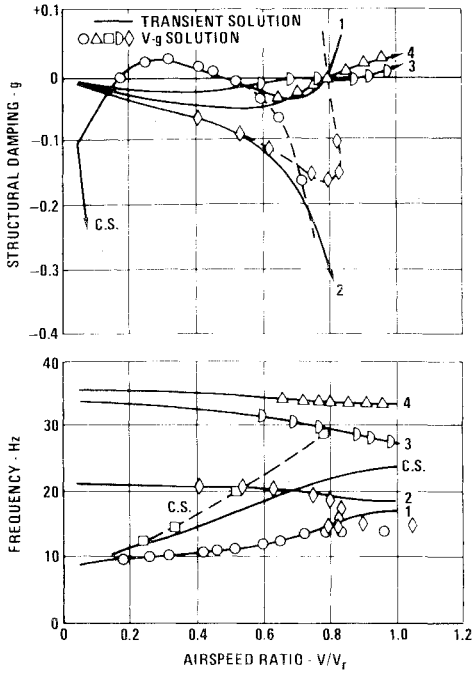

Fig. 5 Comparison of transient and V-g-ω flutter solutions for wing with control surface.

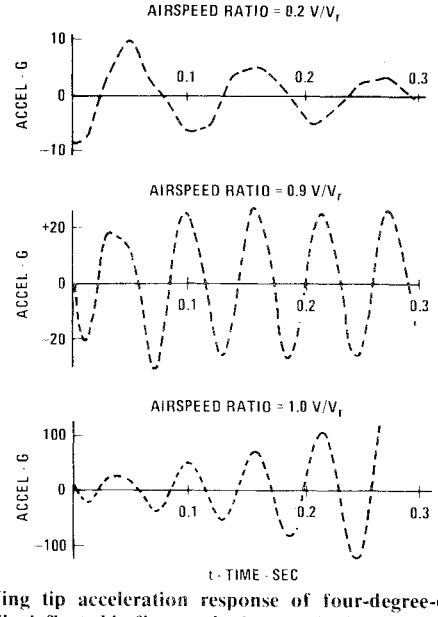

Fig. 6 Wing tip acceleration response of four-degree-of-freedom wing initially deflected in first mode shape and released.

A flutter analysis using five degrees of freedom is presented in Fig. 5. The generalized coordinates are the first four normal wing modes plus rigid control surface rotation. The control surface restraint frequency is 10 Hz. For configurations like this, the transient solution provides information about the real dynamic behavior that the V-g-ω solution cannot provide. For example, at airspeeds greater than 0.8 V/V_r, the control surface frequency is increasing with airspeed at such a rate that this mode fails to cross any more reduced frequency lines; thus, the V-g-ω solution characteristic values for the control surface mode are negative and nonphysical above this airspeed. The transient solution, however, shows the control surface mode involved with the third mode for the 0.9 V/V_r flutter crossing. Note that the second mode V-g-ω results have a loop back with airspeed such that, at 0.8 V/V_r, there are two choices for the frequency of this mode. It is the transient solution that provides the physical description of the

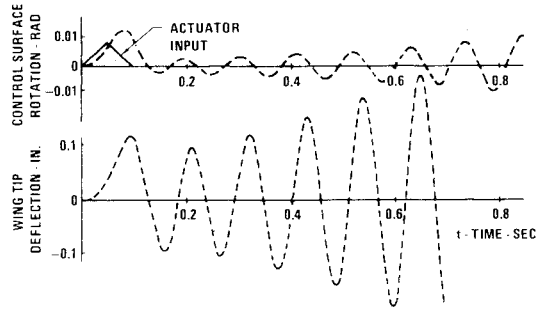

Fig. 7 Time history response of the wing control surface configuration to an actuator input for airspeed ratio of 0.2 V/V_r.

second mode variation with airspeed. At the five neutral stability points of this figure, the transient solution and the V-g-ω solution agree. The results of Figs. 4 and 5 indicate the validity of the transient aerodynamic formulation and its value for transient flutter stability analysis.

Time History Analysis

Time history analyses of the configurations applicable to Figs. 4 and 5 have been performed to validate the time formulation of the transient aerodynamics. The analyses were performed using the MIMAC simulation language described in Ref. 13. Figure 6 presents a solution using the four-degree-of-freedom configuration whose flutter solution was presented in Fig. 4. The configuration initially was deflected in its first mode shape and released. Results are presented for three airspeeds which are stable, neutral, and unstable flutter conditions. The data plotted represent the variation of total aft wing tip acceleration with time. The dynamic behavior shown in Fig. 6 agrees with the flutter analysis.

The time history analysis of Fig. 7 presents a study of the five-degree-of-freedom wing-control surface configuration. In this simulation, the aeroelastic configuration initially is completely at rest. The control surface receives a saw tooth actuator input. Thus, this time history is a solution to the nonhomogeneous differential Eq. (25) with a nonharmonic forcing function F_μ. Because this is a flutter condition (see Fig. 5) and because of the low spring rate of the control surface, the control surface exhibits considerable initial dynamic overresponse to this input. The wing behavior is described by the total aft wing tip deflection which was evaluated from the generalized coordinate time histories. After the initial response to the actuator, the stable modes decay, but the flutter mode diverges, as predicted by the flutter solution.

Concluding Remarks

A numerical method has been presented for evaluation of subsonic transient lifting surface aerodynamics. The separation of the complex generalized aerodynamic forces into stiffness and damping forces has made it possible to formulate relatively simple transfer functions which describe the behavior of each matrix element with remarkable numerical accuracy. The result is a transient aerodynamic data set which has been implemented successfully into the aeroelastic equations of motion with respect to both real time derivatives of the generalized coordinates and Laplace operators. Both of these formulations have been validated by the numerical examples presented.

The equations can be used to evaluate the nonharmonic arbitrary motion of a specific aeroelastic configuration at a constant airspeed and Mach number. Thus, they can be used to develop an analytical model of a flexible aircraft in a variety of dynamic flight situations. The aeroelastic model can be combined with the flight control system for a linear stability analysis using the Laplace operator formulation and for a time history simulation including nonlinearities of the control system. This analysis capability is a requirement for future high-performance aircraft because of larger in-

volvement of the flight control system in optimum performance, loads control, flutter suppression, and ride qualities. The aeroelastic model can be used to simulate dynamic maneuvers for a loads analysis which automatically includes dynamic amplification and inertial relief.

This numerical method uses the results of existing linear unsteady lifting surface programs. Thus, it can be used readily with multiple surface programs and has potential application with supersonic programs. The method has potential application to time simulation of gust response using lifting surface gust loads. It is possible that the transient flutter solution can simplify structural optimization procedures concerned with flutter prevention. This could be accomplished by using a single set of flutter sensitivity parameters evaluated only at the required airspeed.

References

[1]Richardson, J. R., "A More Realistic Method for Routine Flutter Calculations," AIAA Symposium on Structural Dynamics and Aeroelasticity, Cambridge, Mass., Aug. 30 to Sept. 1, 1965.

[2]Rodden, W. P., and Stahl, B., "A Strip Method for Prediction of Damping in Subsonic Wind Tunnel and Flight Flutter Test," *Journal of Aircraft*, Vol. 6, Jan.-Feb, 1969, pp. 9-17.

[3]Ferman, M. A., Burkhart, T. H., and Turner, R. L., "First Quarterly Report for Conceptual Flutter Analysis,", McDonnell Aircraft Co., St. Louis, Mo., Rep. E549, March 1966.

[4]Utterback, F. D., "Model F-4J Airplane Slatted Leading Edge Stabilator Flutter Substantiation Report," McDonnell Aircraft Co., St. Louis, Mo., Rep. E801, Aug. 1966.

[5]Landy, R. J., "A Computer Program for Time Response, Fast Fourier Transform and Adaptive Flutter Control Algorithm for Servoaeroelastic Systems," McDonnell Douglas Corp., St. Louis, Mo., Rep. A2889, May 30, 1974.

[6]Triplett, W. E., Kappus, H. P. F., and Landy, R. J., "Active Flutter Control," *Journal of Aircraft*, Vol. 10, Nov. 1973, p. 669.

[7]Hassig, H. J., "An Approximate True Damping Solution of the Flutter Equations by Determinant Iteration," *Journal of Aircraft*, Vol. 8, Nov. 1971, pp. 885-889.

[8]Rowe, W. S., "Collocation Method for Calculating the Aerodynamic Pressure Distributions on Lifting Surface Oscillating in Subsonic Compressible Flow," AIAA Symposium on Structural Dynamics and Aeroelasticity, Boston, Mass., Aug. 30-Sept. 1, 1965, p. 31.

[9]Cunningham, A. M., "A Rapid and Stable Subsonic Collocation Method for Solving Oscillatory Lifting Surface Problems by the Use of Quadrature Integration," AIAA Paper 70-191, Denver, Colo., 1970.

[10]Albano, E. and Rodden, W., " A Doublet-Lattice Method for Calculating Lift Distributions on Oscillating Surfaces in Subsonic Flow," *AIAA Journal*, Vol. 7, Feb. 1969, pp. 279-285.

[11]Rodden, W. P., Giesing, J. P., and Kalman, T. P., "New Developments and Application of the Subsonic Doublet Lattice Method for Non-Planar Configurations," *Symposium on Unsteady Aerodynamics for Aeroelastic Analysis of Interfering Surfaces*, NATO AGARD CP80, Part II, Nov. 1970, p. 4-1.

[12]Bryson, A.E. and Ho, Y.C., *Applied Optimal Control*, Ginn and Co., 1969, pp. 19-21.

[13]Niesse, D. H., "MIMAC: A Digital System for Continuous Simulation," McDonnell Douglas Automation Co., Rep. MDC-NO108-031, 1971.

[14]System/360 Continuous System Modeling Program User's Manual," GH20-0361-4, IBM Corp.

[15]Burkhart, T. H., "Subsonic Kernel Function Program for Planar Wings with a Control Surface," McDonnell Douglas Co., Rep. EN914, March 1973.